Simple Measurement of Eye Diagram and BER Using High-Speed Asynchronous Sampling

Ippei Shake, *Member, IEEE*, Hidehiko Takara, *Member, IEEE*, and Satoki Kawanishi, *Member, IEEE, Member, OSA*

***Abstract*—This paper discusses eye diagram measurement using asynchronous sampling. Simple bit error rate (BER) estimation from eye diagrams is performed. The use of high-speed asynchronous optoelectrical (OE) sampling enables the monitoring of fixed timing Q-factors to be performed simply.**

***Index Terms*—Asynchronous sampling, bit error rate (BER) estimation, eye diagrams, optoelectrical (OE) sampling, Q-factor, signal quality monitoring.**

I. Introduction

Signal quality monitoring is an important issue in optical transport networks (OTNs) and should satisfy several general requirements [1]–[3]. There are several approaches for this purpose including both digital and analog techniques [1], [4]. In the schemes developed so far, the key weakness is that it takes too long to measure even moderate levels of the system bit error ratio (BER). Solutions include synchronous sampling for fixed timing *Q*-factor (Q_t) measurement [5]–[9] and asynchronous sampling for averaged *Q*-factor $(Q_{\rm avg})$ measurement [10]–[13] or Q_t measurement [14]. The fixed timing *Q*-factor Q_t is the Q-factor at the fixed timing of t as discerned in open eye diagrams. Asynchronous sampling dispenses with timing extraction, so asynchronous sampling techniques are transparent to the bit rate and signal format. However, a correlation factor or complicated software calculations are needed to obtain the BER. Moreover, electrical and optical sampling techniques used in all such schemes reported to date are expensive and complicated.

This paper precisely discusses a simple Q_t monitoring method that we previously proposed [15] that utilizes the open eye diagrams captured by asynchronous sampling. In Section II, a setting procedure for the local sampling clock frequency and the influence of sampling clock frequency inaccuracy and signal wander for high-speed sampling are discussed. Then, a signal quality monitoring circuit using an optoelectrical (OE) sampling technique is described in Section III. Finally, the experimental results and a discussion of the results are presented in Section IV.

The BER is easily and accurately obtained from Q_t. We introduce a Q_t measurement procedure and a simple signal quality monitoring circuit that employs a high-speed asynchronous optoelectrical sampling technique for bit rates of 10 Gb/s. OE sampling allows the optical signal to be gated by an electrical pulse. We use an electroabsorption (EA) modulator as the sampling device. OE sampling makes it possible to achieve simple high-speed sampling, which realizes Q_t evaluation using a simple circuit and simple software calculations.

II. Eye Diagram Measurement With Asynchronous Sampling

A. Setting of Local Sampling Clock Frequency

Here, we discuss eye diagram measurement using the asynchronous sampling technique. We discuss the setting of the local sampling clock frequency f_c in detail. The repetition frequency of f_c is determined based only on the number $(n/m)f_s$, which is related to the optical signal bit rate, f_s, and is not made to follow the bit phase of the optical signal using clock extraction or the like. For example, cases in which the optical signal bit rate is 2.5, 10, or 40 Gb/s are considered. In these cases, if 100 MHz, a common measure of these bit rates, is assumed as the information required to determine the repetition frequency of the sampling clock, f_c can be determined and set to 100 MHz $\pm a$ Hz, where a is the offset frequency. In other words, if we set the sampling clock frequency to 100 MHz $\pm a$ Hz, which is known in advance as information concerning the signal bit rate, the sampling system can be applied to signals whose bit rate is a common multiple of 100 MHz. In another case, we can certainly assume some knowledge of f_s such as the data format (e.g., SONET/SDH, OTN (digital wrapper), Ethernet, etc.) since such information is relatively easy to obtain. Moreover, it is possible to set f_c without such information concerning f_s as long as we can sweep and adjust f_c to ensure that the measured eye diagrams are open.

Regarding the display of the eye diagrams, the sampled data can be displayed on a display device without alteration, in the order in which the data were sampled. In such a case, instead of arranging every sampled point in a time series, the sampled points may be superposed from time zero over a specified interval. An eye-diagram can be displayed by repeating this process for every sampled point. The superposition period is described below. Here, a case is described in which the bit rate of the data signal is f_s, and the repetition frequency f_c of the sampling pulse is represented by

$$f_c = \frac{n}{m} f_s \pm a \tag{1}$$

where n and m are natural numbers, and a is the offset frequency. In the conventional synchronous sampling technique,

Manuscript received September 2, 2003; revised February 11, 2004.

The authors are with NTT Network Innovation Laboratories, NTT Corporation, Kanagawa 239-0847, Japan (e-mail: shake.ippei@lab.ntt.co.jp).

Digital Object Identifier 10.1109/JLT.2004.827669

f_c is determined through hardware synchronization with f_s and by satisfying

$$T_{\text{step}} = \frac{1}{f_c} - \frac{1}{\left(\frac{n}{m}\right) f_s} = \frac{1}{k f_s} \tag{2}$$

where T_{step} is the sampling time interval and k is the number of sampling points per time slot of the signal. From (2), f_c is given as

$$f_c = \frac{f_s}{\frac{1}{k} + \frac{m}{n}}. \tag{3}$$

Comparing (1) to (3), a is determined as

$$a = \frac{\left(\frac{n}{m}\right)^2}{k + \left(\frac{n}{m}\right)} f_s. \tag{4}$$

If we use the asynchronous sampling technique, a is not accurately determined, and will satisfy the following condition

$$\frac{\left(\frac{n}{m}\right)^2}{k + \left(\frac{n}{m}\right)} f_s \le a < \frac{\left(\frac{n}{m}\right)^2}{k - 1 + \left(\frac{n}{m}\right)} f_s \tag{5}$$

where k is a natural number. Here, n/m is a value pertaining to the ratio between f_s and f_c. For example, if n/m is $1/100$ and f_s is 10 Gb/s, f_c is set to approximately 100 MHz, showing that the sampling frequency is such that one sampled point is obtained for approximately every 100 bits of the data signal. Furthermore, k is a value relating to the superposition period, indicating that sampled points are superposed in units of k. As an example, plot examples of points P1 to P8 each corresponding to a section of the sampled data are described below for a case where $f_c = (n/m) f_s - a$, with reference to Fig. 1(a), (b), and (c). Fig. 1(a) is a diagram showing the waveform of a data signal [although only points P1 to P5 are shown in Fig. 1(a)]. Fig. 1(b) and (c) are diagrams showing plot examples. The offset frequency, a, should satisfy (5), and Fig. 1(c) is a particular case when a satisfies (4).

Generally, we should consider when

$$a \ne \frac{\left(\frac{n}{m}\right)^2}{k + \left(\frac{n}{m}\right)} f_s. \tag{6}$$

Furthermore, in this example, the variables satisfy $n/m = 1$ and $k = 4$.

In the case above, the value of offset frequency $a (= f_s - f_c)$ is within the range of

$$\frac{1}{5} f_s \le a < \frac{1}{4} f_s. \tag{7}$$

In the other words, if we set $T_{\text{step}} (= (1/f_c) - (1/f_s))$

$$\frac{1}{4 f_s} \le T_{\text{step}} < \frac{1}{3 f_s}. \tag{8}$$

T_{step} is set to a value greater than $1/4$ and less than $1/3$ of one timeslot which is the reciprocal of f_s. The waveform within one timeslot is reproduced by arranging points P1 to P4 in order [Fig. 1(b)]. In this example, point P5 is not plotted in a position following point P4, and is instead plotted after returning to time zero. Here, the superposition method is used. The superposition method involves aligning the time position of point P5 with the time position of point P1, as shown in Fig. 1(b). When the time position of point P5 is aligned to the time position of point P1, the second superposed waveform presents slight temporal deviation relative to the first waveform. In superposing the third and then fourth waveforms in the same manner, the degree of deviation increases gradually, and consequently the eye tends toward closing as the number of superposed waveforms increases. The only information required to realize this superposition is the value of n/m. Because the sampling clock can be set locally, k can be determined arbitrarily within the range of natural numbers, and it can be said that a larger value is preferable for the reproduction of a complicated waveform.

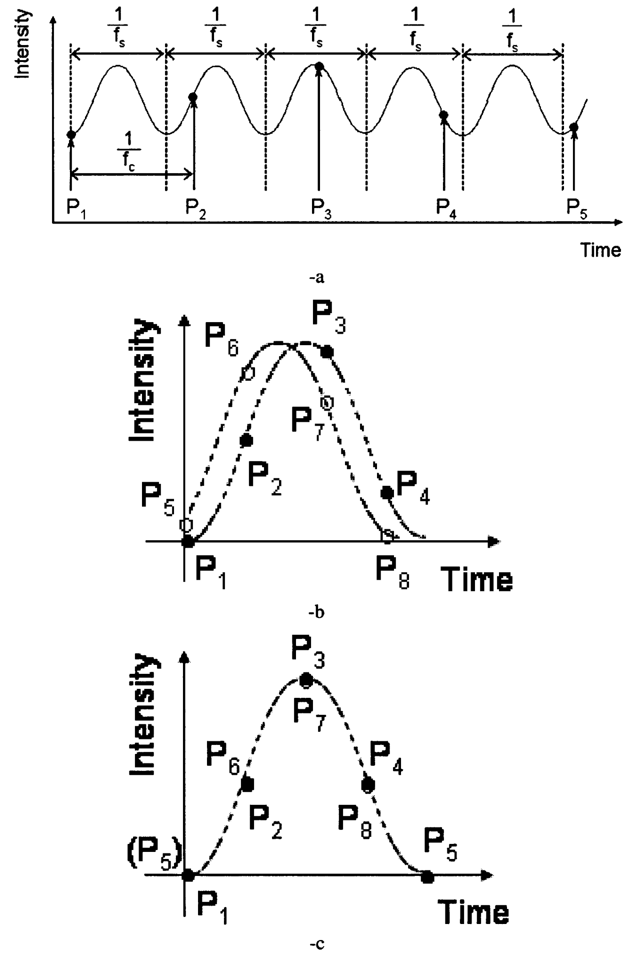

Fig. 1. (a) Signal waveform and sampling examples. (b) Diagrams showing plot examples (when a satisfies (5), $a \ne ((n/m)^2)/(k + (n/m)) f_s$). (c) Diagrams showing plot examples (when $a = ((n/m)^2)/(k + (n/m)) f_s$).

First, we estimate the deviation that occurs when the time position of point P5 is aligned to the same time position as point P1. If a equals $(1/4) f_s$, point P5 is aligned to point P1 at a period of $1/f_s$. Consequently if superposition is performed in units of four points (or if superposition is performed based on a multiple of four), no deviation occurs in the superposing of the second waveform. However, a generally deviates slightly from $(1/4) f_s$ because clock recovery is not used for setting f_c, as is apparent from the equation above used to define the range of a.

Here, assuming that z is a real number that satisfies

$$k-1 < z \leq k \tag{9}$$

then

$$a = \frac{\left(\frac{n}{m}\right)^2}{z + \left(\frac{n}{m}\right)} f_s \tag{10}$$

and because in the current case $n/m = 1, z$ is a real number that satisfies $3 < z \leq 4$; therefore

$$a = \frac{1}{z+1} f_s. \tag{11}$$

Performing the calculations based on these facts shows that in comparison with a case where $a = (1/4) f_s$, the size of the deviation $k\Delta T_{\mathrm{step}}$, which occurs when superposing waveforms, is

$$k\Delta T_{\mathrm{step}} = \frac{k-z}{z f_s} \tag{12}$$

where ΔT_{step} is the time difference of the sampling time interval between when a satisfies (4) and when a satisfies (10). The value of $k\Delta T_{\mathrm{step}}$ becomes the deviation of each superposing waveform. In other words, as the waveforms are superposed a second and a third time, and so on, each waveform deviates by an additional $k\Delta T_{\mathrm{step}}$ in the time domain. Once the total deviation equals half the size of a timeslot which is the reciprocal of f_s, the eye diagrams become completely closed, and as such this is the upper limit for deviation. If the number of sampled points to be measured at a time is deemed N_{samp}, and the number of superposition is deemed j, then

$$kj \leq N_{\mathrm{samp}}. \tag{13}$$

Accordingly, if the total accumulated deviation is deemed $\mathrm{Sum}[k\Delta T_{\mathrm{step}}]$, then

$$\mathrm{Sum}[k\Delta T_{\mathrm{step}}] = \frac{(k-z)j}{z f_s}. \tag{14}$$

Here, we consider measurement of a nonreturn-to-zero (NRZ) signal, whose rise and fall times after measurement using this method are equal to or less than half of $1/f_s$. Because the condition enabling eye opening evaluation $\mathrm{Sum}[k\Delta T_{\mathrm{step}}]$ is equal to or less than half of $1/f_s$, if the number of sampled points is within a range which satisfies

$$\frac{(k-z)j}{z f_s} \leq \frac{1}{2 f_s} \tag{15}$$

that is

$$j \leq \frac{z}{2(k-z)} \tag{16}$$

then the eye opening can be evaluated even if a local clock is used.

B. Influence of Sampling Clock Frequency Detuning and Signal Wander on High-Speed Sampling

In the previous subsection, we described the setting of the local sampling clock frequency and the principle of eye diagram monitoring by considering a simple case when $n/m = 1$ and $k = 4$ and by discussing small detuning of the sampling clock frequency. The detuning is the difference between a in (4) and that in (10), and we considered the case only when $k-1 < z \leq k$. This case includes only when the sampling clock frequency detuning is small. In this subsection, we discuss the more general case when the sampling clock frequency detuning is larger.

As discussed in Subsection II-A, to obtain the open eye diagrams, all sampling points are plotted in time order, and superposed every k (or multiple of k) samples. If frequency detuning $|\delta f| = 0, T_{\mathrm{step}}$ satisfies (2). However, here we assume f_s is not accurately known at the signal quality monitoring circuit. For example, some knowledge of f_s such as the data format can be used, but the accurate bit rate cannot be known. Note that when timing extraction is not used, f_s is not accurately known at the signal quality monitoring circuit, so f_c must be decided independently as discussed in Subsection II-A. Moreover, the performance of the sampling clock source causes inaccuracy in the setting of f_c. However, high-speed sampling allows us to obtain open eye diagrams even under this condition, which means that the eye diagram can be evaluated as shown in the following theoretical evaluation. We assume frequency detuning δf due to the inaccuracy in determining f_s and/or f_c. These inaccuracies in f_s and/or f_c cause (2) and (3) to fail.

The time shift of sampling time interval ΔT_{step} due to δf is expressed by using δf as follows:

$$\Delta T_{\mathrm{step}} = \frac{1}{f_c} - \frac{1}{f_c + \delta f}. \tag{17}$$

When $|jk\Delta T_{\mathrm{step}}|$ is $1/(2 f_s)$ or less, the open eye diagram is constructed. Therefore, the following condition must be satisfied.

$$f_c \geq \sqrt{2 f_s jk |\delta f|} \tag{18}$$

where $jk = N_{\mathrm{samp}}$ (j and k are natural number).

For example, when f_s is 10 Gb/s and the frequency detuning $|\delta f|$ is 20 ppm (200 kHz), $N_{\mathrm{samp}}(\sim jk)$ is limited to 250 and the requirement of f_c is 1 GHz or more. In other words, if the sampling clock rate is in the order of 1 GHz, our measurement circuit allows inaccuracy in the setting of f_s and/or f_c to the level of ±200 kHz to capture the open eye diagrams. Therefore, the high-speed asynchronous OE sampling [15] enables us to realize simple *Q*-factor monitoring without complicated software calculations as are demanded with the use of the periodogram [14]. If $|\delta f|$ can be reduced by obtaining more accurate information concerning signal bit rate f_s or by sweeping and adjusting sampling clock rate f_c, the order of the sampling clock rate can be reduced and N_{samp} can be increased, as long as the influence of the signal wander is negligible based on the following discussion.

Signal wander is sometimes estimated from the group delay due to a change in the transmission fiber caused by temperature fluctuations. When the total sampling number is N_{samp} points, the transmission fiber length is L m, temperature change is δT°C/s, and the group delay coefficient of optical fibers is α

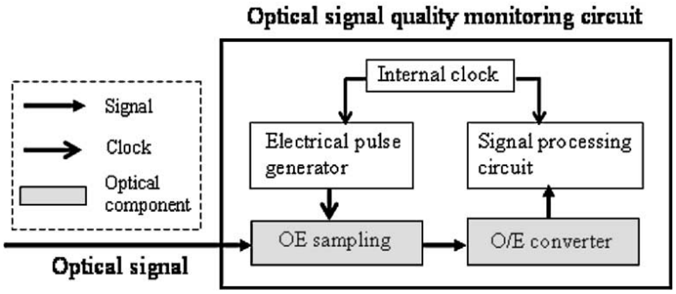

Fig. 2. Block diagrams of signal quality monitoring circuit using asynchronous OE sampling.

ps/m/°C. The total group delay per total sampling time $\Delta t_{\mathrm{wander}}$ satisfies

$$\Delta t_{\mathrm{wander}} = \alpha \frac{N_{\mathrm{samp}}}{f_c} L\delta T. \tag{19}$$

For example, when α is 0.2 ps/m/°C (measured value), N_{samp} is 250, L is 320×10^3 m, δT is 0.5×10^{-3} °C/s (20 °C per 12 h), f_c is approximately 1 GHz, and $\Delta t_{\mathrm{wander}}$ is approximately 8×10^{-6} ps, which is sufficiently small to measure the open eye diagrams without timing extraction.

III. Signal Quality Monitoring Circuit Using Optoelectrical Sampling

The optical signal quality monitoring circuit consists of an OE sampling module, an internal clock source, an electrical pulse generator, an O/E converter, and a signal processing circuit as shown in Fig. 2. OE sampling means optical gating with electrical pulses. The repetition rate of the electrical pulses is approximately 100 MHz or 1 GHz. An EA modulator is used as the OE sampling module. The EA modulator and electrical pulse generator are relatively small and simple compared to conventional optical sampling components or electrical high-speed sampling modules. In the conventional electrical sampling case, the O/E converter bandwidth should be wider than that of the signal bit rate. On the other hand, in the OE sampling method, the signal is optically sampled at a repetition rate lower than the signal bit rate. Therefore, the O/E converter bandwidth is narrower than the signal bit rate. The signal processing circuit analyzes the sampled signal to determine the *Q*-factor at fixed timing phase $t(Q_t)$, and estimates the BER.

Using the aforementioned technique, we constructed an optical signal quality monitoring prototype. A polarization-independent EA modulator with a 40-GHz bandwidth was used to achieve polarization-independent operation. Time resolution is less than 24 ps when the OE sampling repetition rate is 100 MHz, which is suitable for 10 Gb/s optical signals. The time resolution can range up to 8 ps when the OE sampling repetition rate is 1 GHz. In this case, the signal bit rate can range up to 40 Gb/s. In our measurement circuit, the bandwidth of the signal processing circuit is not sufficient to deal with 8 ps time resolution, so the experiment is performed using a 10 Gb/s optical signal and 24 ps time resolution. We also measured the wavelength dependence of the *Q* factor. The bandwidth allowing a 2-dB decrease from the maximum *Q*-factor value was 40 nm (from 1543 to 1583 nm). This range was limited by the characteristics of the EA modulator used. By shifting the center wavelength to 1550 nm, the entire C-band can be covered. The major specifications are summarized in Table I.

TABLE I
Specifications of Signal Quality Monitoring Circuit

Parameters	Measured value
Sampling rate	100 MHz to 1 GHz
Time resolution	< 24 ps
Signal bit rate	< 10.7 Gbit/s
Wavelength range	>40 nm (1543-1583 nm)
Available input power	-5.0 to +5.0 dBm
Polarization dependence	< 1.0 dB

The technical point here is that the EA modulator and electrical pulse generator achieve high-speed sampling with a high degree of time resolution. Moreover, they are small and relatively cost effective compared to conventional optical sampling components or an electrical high-speed sampling module. The O/E converter uses an avalanche photo diode with a 2.5-GHz bandwidth. Since the signal is sampled optically, the requirements for the O/E converter bandwidth are not so strict compared to the electrical sampling case, and it is possible to measure exact waveforms without ringing of wide-bandwidth O/E converters. At the signal processing circuit, the sampled signal is calculated and the *Q* factor at fixed timing t (Q_t) is estimated [15]. The graphical user interface of our prototype is shown in Fig. 3.

IV. Experiment and Discussion

A. Q_t Monitoring

Parameter Q_t is estimated from the open eye diagrams captured by the asynchronous sampling aforementioned. An example of the eye diagrams, the amplitude histograms at fixed timing phase t, and Q_t are shown in Fig. 3. Parameter Q_t is defined by

$$Q_t = \frac{|\mu_1 - \mu_0|}{\sigma_1 + \sigma_0} \tag{20}$$

where μ_i and σ_i are the mean and standard deviations of the mark $(\mathrm{i}=1)$ and space $(\mathrm{i}=0)$ level distributions of the amplitude histograms, respectively. The midpoint of the timing phase between the two white lines in Fig. 3 is t and the sampling points between the two white lines are used in the estimation.

Fig. 4 shows the asynchronous eye diagrams when the detuning of sampling frequency δf is 6 kHz. Both the 10-Gb/s NRZ (left figures) and RZ (right figures) optical signal (40 ps pulse width) are measured. The eye diagrams at the top of Fig. 4 represent when the total number of sampling points N_{samp} is 1000 points. The subsequent sets of figures are for $N_{\mathrm{samp}} = 2000, 4000, 8000$, and $16\,000$ points. For the NRZ signal, $N_{\mathrm{samp}} = 8000$ seems to be the limit to evaluate Q_t. Whereas, the rise and fall time of the NRZ signal at the measurement circuit is approximately half of $1/f_s$, so (18) can be applied to the eye diagram. Therefore, the limit of N_{samp} becomes $N_{\mathrm{samp}} \le 8300$, where $f_c \sim 1$ GHz (time resolution

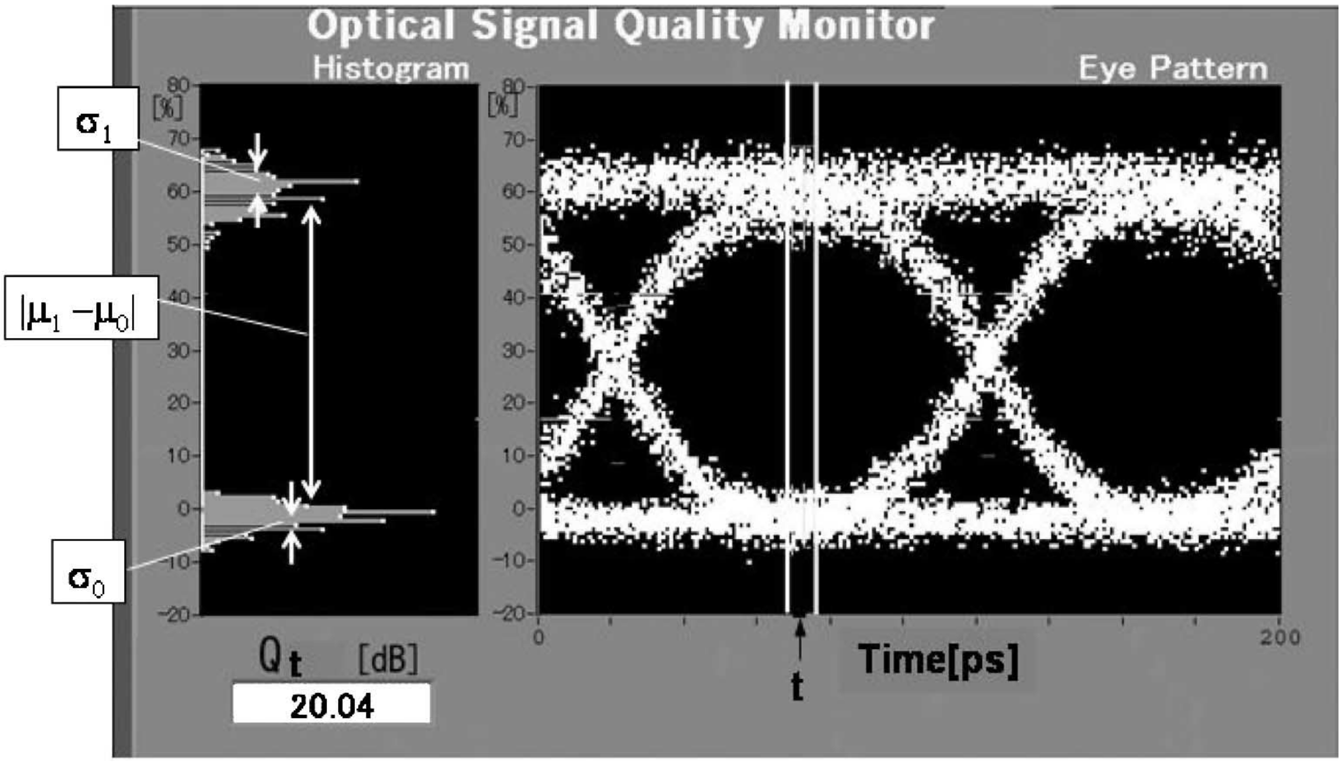

Fig. 3. Measured eye diagrams of 10 Gb/s NRZ optical signal and amplitude histograms at fixed timing phase t.

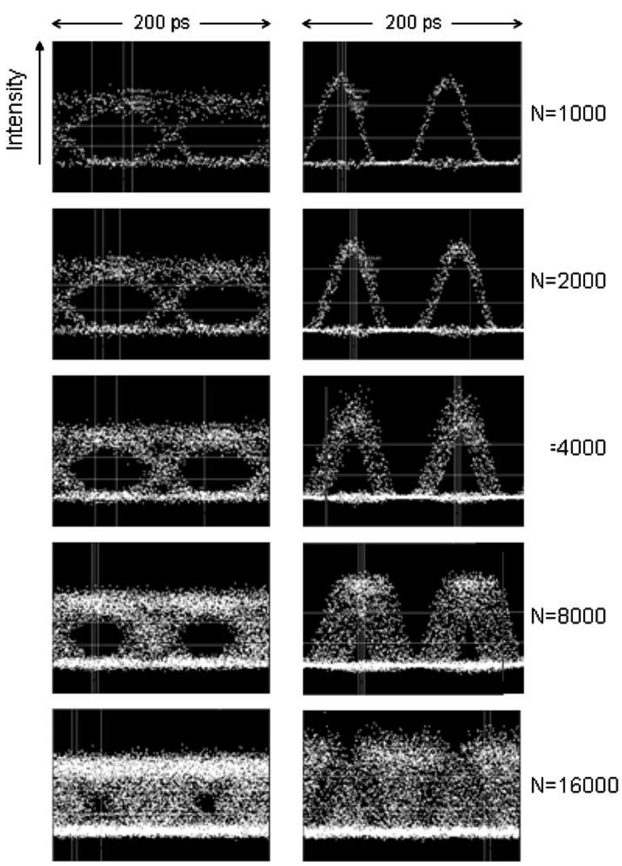

Fig. 4. Asynchronous eye diagrams when detuning of sampling frequency δf is 6 kHz for (Left) 10 Gb/s NRZ signal, (Right) 10 Gb/s RZ signal: total sampling points $N_{\rm samp}$ is changed [1000 points (top), 2000, 4000, 8000, 16 000 (bottom)].

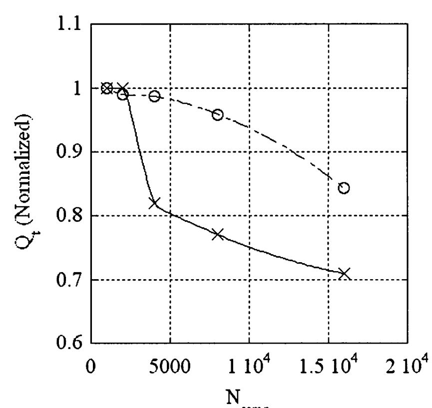

Fig. 5. Relationship between Q_t and $N_{\rm samp}$ when detuning of sampling frequency δf is 6 kHz for 10 Gb/s NRZ signal (Circles) and 10 Gb/s RZ signal (Crosses). Q_t is normalized by the values when $N_{\rm samp} = 1000$.

$\sim$24 ps), $|\delta f| \sim 6$ kHz and $f_s = 10$ Gb/s, and this is consistent with the results of the NRZ signal in Fig. 4. The relationship between Q_t and $N_{\rm samp}$ is shown in Fig. 5. For the NRZ signal, Q_t starts to fall when $N_{\rm samp}$ is over 5000. At the point when $N_{\rm samp}$ is 8000, Q_t is slightly reduced. This is because sampling points for calculating Q_t are obtained from the area of $1/5 \times T_{\rm slot}$ (time slot) and some cross points are considered (see next subsection).

On the other hand, the situation of the RZ signal is different from the NRZ signal. Because the RZ signal has a very narrow mark level distribution (that is, the time region of the mark level is very small), the limit of $N_{\rm samp}\}$ when $|\delta f| \neq 0$ becomes smaller than that for the NRZ signal. In Fig. 4, $N_{\rm samp} = 2000$

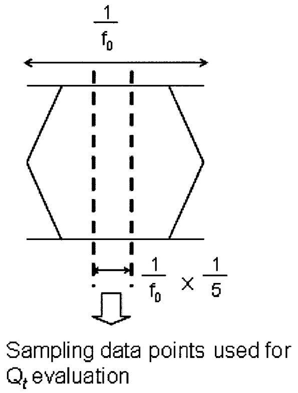

Fig. 6. Sampling data points used for Q_t evaluation.

seems to be the upper limit of the total number of sampling points, and this is $1/4$ that of the NRZ signal. The same result is shown in Fig. 5. This factor depends on the pulse width of the RZ optical signal and the time resolution of the signal quality monitoring circuit.

If we need more sampling points than the limit to evaluate Q_t, we can choose two provisions. One is to sweep f_c to reduce the $|\delta f|$ as it approaches 0. The other is to repeat N_{samp} sampling several times but less than the limit, and superimpose the eye diagrams arranging the maximum eye opening phase into the same time phase.

B. Q_t Measurement Reliability

The measurement reliability means whether the Q_t value is uniformly evaluated when the optical signal quality does not change. This characteristic is represented by the parameter of the variation of multiple measurements.

The variations of the measured Q_t and Q are defined as ΔQ_t and ΔQ, respectively, and the linear fitting slope of Q_t versus Q is defined as slope, where $\Delta Q_t, \Delta Q$, and slope are the parameters of measurement reliability. As discussed in [3], these parameters are easily recognized and ΔQ becomes

$$\Delta Q = \frac{\Delta Q_t}{\text{slope}}. \tag{21}$$

The measurement reliability depends on N_{samp} of the signal quality monitoring circuit. Fig. 7 shows the dependence of the variation of multiple measurements on sampling data points used in the Q_t evaluation. The sampling points used for the Q_t calculation are now set to the points in one-fifth of time slots T_{slots} (Fig. 6). Since all sampling points are plotted in time order and are superposed on every time slot (which equals k samples), the number of sampling points in $1/5 \times T_{\text{slot}}$ equals $1/5 \times N_{\text{samp}}$. The vertical axis shows the standard deviation of 10 measurement points, which pertain to ΔQ_t in (21).

The more the number of samplings, N_{samp}, increases, the lower the standard deviation of the 10 measurement points becomes. For the Q_t evaluation technique, the value of the *slope* is expected to be one. So we can design parameter N_{samp} from (21) and Fig. 7. When the required value of ΔQ is less than 0.60, which corresponds to the difference in BER between 10^{-10} and $10^{-9}, \Delta Q_t$ must also be less than 0.60. Parameter ΔQ_t is defined as $2 \times$ (standard deviation), the permitted standard deviation value is less than 0.30. The N_{samp} value to maintain the measurement reliability is defined from Fig. 7 as more than 25 000 points.

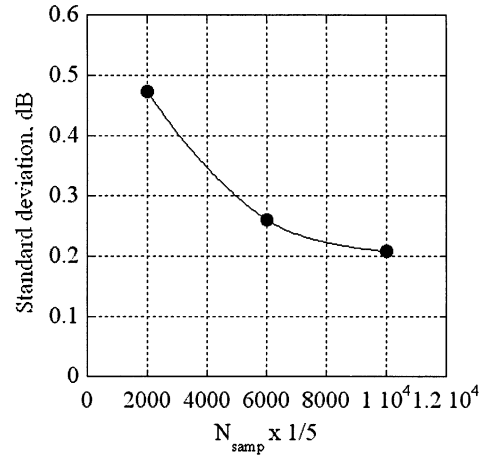

Fig. 7. Dependence of the standard deviation for ten measurement points of Q_t on N_{samp}: 10 Gb/s NRZ signal, $Q = 16$ dB (BER $\sim 10^{-10}$).

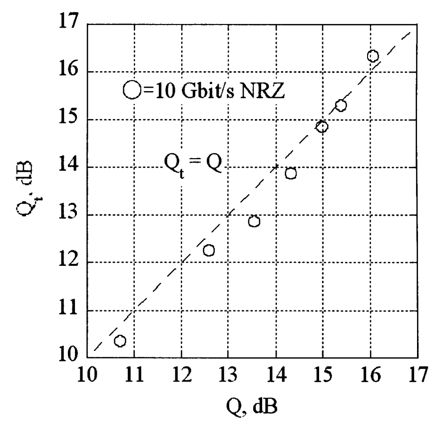

Fig. 8. The relationship between Q_t and Q for 10 Gb/s NRZ signal.

C. Q_t Measurement for Simple BER Estimation

We confirm the applicability of the signal quality monitoring circuit to the BER estimation. Parameter Q_t is obtained by using the procedure described in the previous section, and parameter Q is derived from the measured BER using the Gaussian assumption. We set t at the time when the measured eye diagram is the most widely open. In regard to local sampling clock frequency f_c, we sweep the value and adjust to $|\delta f| = 0$. The values of N_{samp} are set to 30 000 based on the discussion in the previous section.

Fig. 8 shows the relationship between Q_t and Q for 10 and 40 Gb/s NRZ optical signals at different signal optical signal-to-noise ratio (OSNR) values. Good relationships are recognized in the figure, and the slope of the relationship equals one, regardless of the signal bit rate. Note that the values of Q_t basically equal those of Q. This means that it is possible to discern the BER value directly if we estimate Q_t. For instance, when the measured Q_t value is 16.4 for a 10 Gb/s optical signal, the BER of the signal is recognized to be 10^{-10}.

The largest Q value we measured is 16.4 dB, which corresponds to the BER of 10^{-10}. Lower BER measurement takes a very long time, so it is difficult to estimate the upper limit of the applicable region of the method. However, since the Q_t measurement is sensitive up to 20 dB (see Fig. 3) it is expected that the BER estimation method using the signal quality monitoring circuit can be applied to $Q = 20$ dB, which corresponds to the BER of 10^{-24}.

V. Summary

We presented a discussion concerning a simple eye diagram measurement using asynchronous sampling. We examined the requirement for sampling clock frequency used locally. We also introduced a signal quality monitoring circuit that uses high-speed asynchronous OE sampling, and experimentally confirmed its ability to estimate the BER for 10-Gb/s NRZ signals. We used a fixed timing Q-factor (Q_t) evaluation procedure that uses open eye diagrams captured by asynchronous sampling. This technique and circuit will form a powerful solution to the performance monitoring requirements of future optical networks.

Acknowledgment

The authors thank M. Kawachi, H. Ichikawa, and K.-I. Sato for their encouragement.

References

[1] G. Bendelli, C. Cavazzoni, R. Girardi, and R. Lano, “Optical performance monitoring techniques,” in *Proc. 26th Euro. Conf. Opt. Commun. (ECOC2000.)*, vol. 4, 2000, pp. 113–116.

[2] R. Giles, “Monitoring the Optical Network,” in *Proc. Symp. Optical Fiber Measurement*, 2002, pp. 19–24.

[3] I. Shake and H. Takara, “Averaged Q-factor method using amplitude histogram evaluation for transparent monitoring of optical signal-to-noise ratio degradation in optical transmission system,” *J. Lightwave Technol.*, vol. 20, pp. 1367–1373, 2002.

[4] ——, Transparent and flexible performance monitoring using amplitude histogram method, in Optical Fiber Communication Conference 2002 (OFC2002), 2002. TuE1.

[5] S. Ohteru and N. Takachio, “Optical signal quality monitor using direct Q-factor measurement,” *IEEE Photon. Technol. Lett.*, vol. 11, pp. 1307–1309, 1999.

[6] C. Schmidt, C. Schubert, J. Berger, M. Kroh, H.-J. Ehrke, E. Dietrich, C. Borner, R. Ludwig, and H. G. Weber, “Optical Q-factor monitoring at 160 Gb/s using an optical sampling system in an 80 km transmission experiment,” in *Proc. Conf. Lasers and Electro-Optics 2002 (CLEO 2002.)*, 2002, pp. 579–580.

[7] S. Norimatsu and M. Maruoka, “Accurate Q-factor estimation of optically amplified systems in the presence of waveform distortion,” *J. Lightwave Technol.*, vol. 20, pp. 19–29, 2002.

[8] M. Westlund, H. Sunnerud, M. Karlsson, J. Hansryd, J. Li, P. O. Hedekvist, and P. A. Andrekson, “All-optical synchronous Q-measurements for ultra-high speed transmission systems,” in *Proc. Optical Fiber Communication Conf. 2002 (OFC2002)*, 2002. Paper ThU2.

[9] C. M. Weinert, C. Caspar, M. Konitzer, and M. Rohde, “Histogram method for identification and evaluation of crosstalk,” *Electron. Lett.*, vol. 36, no. 6, 2000.

[10] I. Shake, H. Takara, S. Kawanishi, and Y. Yamabayashi, “Optical signal quality monitoring method based on optical sampling,” *Electron. Lett.*, vol. 34, no. 22, pp. 2152–2154, 1998.

[11] N. Hanik, A. Gladisch, C. Caspar, and B. Strebel, “Application of amplitude histograms to monitor performance of optical channels,” *Electron. Lett.*, vol. 35, no. 5, pp. 403–404, 1999.

[12] M. Rasztovits-Wiech, K. Studer, and W. R. Leeb, “Bit error probability estimation algorithm for signal supervision in all-optical networks,” *Electron. Lett.*, vol. 35, no. 20, pp. 1754–1755, 1999.

[13] C. M. Weinert, C. Schmidt, and H. G. Weber, Application of asynchronous amplitude histograms for performance monitoring of RZ signals, in Proc. OFC2001, 2002. WDD41.

[14] L. Noirie, F. Cerou, G. Moustakides, O. Audouin, and P. Peloso, New transparent optical monitoring of the eye and BER using asynchronous under-sampling of the signal, in Proc. ECOC2002. PD 2.2.

[15] I. Shake, H. Takara, and S. Kawanishi, “Simple Q factor monitoring for BER estimation using opened eye diagrams captured by high-speed asynchronous electrooptical sampling,” *IEEE Photon. Technol. Lett.*, vol. 15, pp. 620–622, 2003.

Ippei Shake (M’02) was born in Kobe, Japan, in 1970. He received the B.S. and M.S. degrees in physics from Kyoto University, Kyoto, Japan, in 1994 and 1996, respectively.

He joined NTT Optical Network System Laboratories, NTT Corporation, Yokosuka, Japan, in 1996. Since then, he has been engaged in research and development of high-speed optical signal processing and high-speed optical transmission systems. He is currently with NTT Network Innovation Laboratories, Kanagawa, Japan. His research interests also include optical networks, optical performance monitoring, and optical time-division-multiplexing/demultiplexing circuits.

Mr. Shake is a Member of the Institute of Electronics, Information and Communication Engineers (IEICE) of Japan.

Hidehiko Takara (M’03) was born in Okinawa, Japan, on November 7, 1962. He received the B.S., M.E., and Ph.D. degrees in electrical engineering from the University of Keio, Kanagawa, Japan, in 1986, 1988, and 1997, respectively.

He joined NTT Transmission Systems Laboratories, Kanagawa, Japan, in 1988. Since then, he has been engaged in research on ultrahigh-speed/large-capacity optical transmission systems and optical measurement techniques. Presently, he is a Senior Research Engineer in NTT Network Innovation Laboratories, NTT Corporation, Kanagawa, Japan.

Dr. Takara is a Member of the Institute of Electronics, Information and Communication Engineers (IEICE) of Japan. He received a paper award from IEICE in 1993 and was awarded the Kenjiro Sakurai Memorial Prize from OEIDA in 1996 and the Electronics Letters Premium from the Institution of Electrical Engineers (IEE) in 1997.

Satoki Kawanishi (S’81–M’83) received the B.E., M.E., and Ph.D. degrees in electronic engineering from University of Tokyo, Tokyo, Japan, in 1981, 1983, and 1993, respectively.

He joined the Yokosuka Electrical Communication Laboratory, Nippon Telegraph and Telephone Public Corporation, Kanagawa, Japan, in 1983, where he has been engaged in research and development of high-speed optical transmission systems and optical signal processing using photonic crystal fiber. He is now with the Photonic Transport Network Laboratory, NTT Network Innovation Laboratories, Kanagawa, Japan.

Dr. Kawanishi is a Member of the Optical Society of America (OSA), the Institute of Electronics, Information and Communication Engineers (IEICE) of Japan, and the Japan Society of Applied Physics. He received the Paper Awards from the IEICE in 1993 and 1995, an achievement award from the IEICE, and Sakurai Memorial Award in 1996.